

A new methodology of studying the dynamics of water sorption/desorption under real operating conditions of adsorption heat pumps: Modelling of coupled heat and mass transfer in a single adsorbent grain

B.N. Okunev^{a,*}, A.P. Gromov^a, L.I. Heifets^a, Yu.I. Aristov^b

^a *Moscow State University, Chemical Department, 119992 Vorobievi Gori, Moscow, Russia*

^b *Borshkov Institute of Catalysis, Pr. Lavrentieva, 5, Novosibirsk 630090, Russia*

Received 23 January 2007; received in revised form 26 February 2007

Available online 11 June 2007

Abstract

A new experimental methodology of studying the kinetics of water vapour sorption/desorption under operating conditions typical for isobaric stages of adsorption heat pumps has been proposed and tested experimentally in [Yu.I. Aristov, B. Dawoud, I.S. Glaznev, A. Elyas, A new methodology to study the kinetics of water vapour sorption/desorption under real operating conditions of adsorption heat pumps: 1. Experiment, *Int. J. Heat Mass Transfer*, submitted for publication]. Here, we analysed results obtained in [Yu et al., submitted for publication] by mathematical modelling of the coupled heat and mass transfer in a single adsorbent grain which is in thermal contact with a metal plate subjected to a fast temperature jump/drop (at constant vapour pressure). The dynamic behaviour turns out to be closely linked with equilibrium properties of the adsorbent, in particular, with the initial/final temperatures and with the shape of the segment of water sorption isobar (convex or concave) between these temperatures.

© 2007 Elsevier Ltd. All rights reserved.

Keywords: Mathematical modelling; Coupled heat and mass transfer; Sorption kinetics; Selective water sorbent; Calcium chloride and silica gel adsorption heat pumps

1. Introduction

A new methodology of studying the kinetics of water vapour sorption/desorption under operating conditions typical for isobaric stages of sorption heat pumps has been proposed and tested experimentally in [1]. The measurements have been carried out on pellets of composite sorbent SWS-1L (CaCl₂ in silica KSK) placed on a metal plate. The temperature of the plate was changed as it takes place in real sorption heat pumps, while the vapour pressure over the sorbent was maintained almost constant (saturation pressures corresponding to evaporator temper-

atures of 5 and 10 °C and condenser temperatures of 30 and 35 °C). The quasi-exponential behaviour of water uptake on time was found for most of the experimental runs. The characteristic time τ of isobaric adsorption (desorption) was measured for one layer of loose grains of 1.4–1.6 mm in size for different boundary conditions of adsorption heat pumps. This approach allows a direct measurement of the temporal evolution of average water uptake under conditions, which closely simulate the scenario of temperature jump or drop in real adsorption heat pumps and refrigerators with a layer of loose grains [2,3]. Such jump is a driving force of water desorption/adsorption during isobaric stages of the cycle of these units.

The only values directly measured according to this methodology are the temperature T of the metal plate and the vapor pressure P over the sample. The average

* Corresponding author. Tel.: +7 495 939 46 49; fax: +7 495 939 33 16.
E-mail address: okunev@tech.chem.msu.ru (B.N. Okunev).

Nomenclature

D_e	efficient pore diffusivity (m ² /s)
k	rate constant (s ⁻¹)
m	mass (kg)
N	water loading (mol _{H₂O} /mol _{CaCl₂})
P	pressure (Pa)
R_p	radius of the adsorbent particle (m)
R	gas constant (J/mol K)
t	time (s)
T	temperature (K)
x	weight portion of CaCl ₂ in the adsorbent (kg/kg)

Greek symbols

α_p	heat transfer coefficient between ambient gas and adsorbent (W/m ² K)
------------	--

ε	void content of the adsorbent particle
ρ	particle density (kg/m ³)
τ	characteristic time (s)
χ	dimensionless differential water loading (–)
λ	thermal conductivity of the adsorbent particle (W/m K)

Subscripts

av	average
f	final value
0	initial value

water uptake as a function of time was calculated from the dependence $P(t)$ [1]. For detailed analysis of temporal evolution of the radial distributions of water uptake, vapour pressure inside the grain and grain temperature (as well as their average values) a detailed mathematical model of the adsorption process is required. Several models have already been reported to describe isothermal and non-isothermal adsorption on a single adsorbent grain [4–9] most of which were summarized in [4]. The aim of all these papers was to study the coupled heat and mass transfer and thermal effects inside the grain by adsorption of vapor.

The reason for the adsorption was assumed to be a fast change in *the gas pressure over the grain*, so that the driving force was the pressure gradient (the gradient of the chemical potential in [8]). The dominant mass transfer resistance was an intraparticle gas diffusion mostly due to molecular and Knudsen mechanisms. Surface diffusion was additionally considered in [8]. The Langmuir and Dubinin equations were used for describing the equilibrium sorption isotherms. Equations developed in these models can be used for describing the coupled heat and mass transfer in the case when the adsorption on single grain is initiated by a fast change in *the plate temperature under the grain* as it is written below. As to our knowledge the adsorption process in a single grain driven by a temperature jump has not been considered before neither by experimental (except [1]) nor by numerical methods.

Here, we present the dynamic model of the water vapour adsorption on a single adsorbent grain being in thermal contact with a metal plate subjected to a fast temperature jump/drop at almost constant vapour pressure. The model takes into account coupled heat and mass transfer in the grain with adsorption processes. This model is used for analysing the experimental results presented in [1] and for understanding links between dynamics and equilibrium of adsorption process.

2. Description of the model

Combined heat and mass transfer in a single adsorbent grain was described by the following system of differential equations:

- (a) the energy balance equation for a single adsorbent grain including the heat of adsorption:

$$\rho_s C_p(T, N, x) \frac{\partial T}{\partial t} - \rho_s \Delta H \frac{x}{\mu_{\text{salt}}} \frac{\partial N}{\partial t} = \lambda_p \Delta T \quad (1)$$

$$0 < r < R_p$$

with the relevant initial and boundary conditions

$$T(r, 0) = T_0,$$

$$\frac{\partial T(0, t)}{\partial r} = 0,$$

$$\alpha_p (T_f - T(R_p, t)) = \lambda_p \frac{\partial T(R_p, t)}{\partial r},$$

where $C_p(T, N, x)$ is the effective heat capacity of the grain [10].

- (b) the mass balance equation including the diffusion of water vapor inside the grain and sorption processes:

$$\frac{\partial C_w}{\partial t} = D_e \Delta C_w - \frac{\rho_s x}{\mu_{\text{salt}} \varepsilon} \frac{\partial N}{\partial t}, \quad (2)$$

$$C_w(r, 0) = \frac{P_0}{RT_0},$$

$$C_w(R_p, t) = \frac{P_0}{RT_f},$$

$$\frac{\partial C_w(0, t)}{\partial r} = 0.$$

We assumed the local adsorption and thermal equilibrium in each point of the grain, the equilibrium uptake $N(T, P_w)$

$[(\text{mol}_{\text{H}_2\text{O}}/\text{mol}_{\text{salt}})]$ at temperature T and pressure P_w being calculated by approximation equations reported in [11].

The pressure P_w inside the grain was calculated as $P_w(r, t) = RT(r, t)C_w(r, t)$. The dimensionless water uptake χ was

$$\chi = \frac{(m(t) - m(0))}{(m(\infty) - m(0))}.$$

The system of differential equation (1)–(2) was numerically solved by methods of runs and iterations including an implicit finite difference method in order to obtain distributions $T(r, t)$, $C_w(r, t)$ and therefore $P_w(r, t)$ and $N(r, t)$. An iso-volumetric discretization in the radial direction was applied as it was done in [12].

The derivative of the uptake with respect to time $\frac{\partial N}{\partial t}$ was transformed as

$$\frac{\partial N}{\partial t} = \frac{\partial N}{\partial F} \frac{\partial F}{\partial T} \frac{\partial T}{\partial t} + \frac{\partial N}{\partial F} \frac{\partial F}{\partial P_w} \frac{\partial P_w}{\partial t},$$

$$F = RT \ln \left(\frac{P_s}{P_w} \right),$$

where F is the free energy of adsorption, P_s is the saturated vapor pressure at temperature T . Terms proportional to the derivative $\frac{\partial N}{\partial t}$ represent the sources of heat (Eq. (1)) and mass (Eq. (2)), respectively, and execute a strong link between the heat and mass transfer processes. Indeed, a local change of temperature due to the heat transfer causes the adsorption (desorption) of water which alters the local vapor pressure. The pressure gradient gives rise to the water diffusion which results in the redistribution of adsorbed water accompanied with the heat release or absorption and so on.

2.1. Analysis of the experimental data

Figs. 1 and 2 show the average dimensionless uptake calculated as a function of time for a single grain of SWS-1L (1.4–1.6 mm size) under conditions equal to those for experimental runs 1 (desorption) and 2 (adsorption) reported in [1]. Good agreement between experimental and calculated uptake curves was obtained with the best fit corresponding to the efficient pore diffusivity $D_e = 3.0 \times 10^{-6} \text{ m}^2/\text{s}$ and the efficient coefficient of heat transfer $\alpha_p = 60 \text{ W}/(\text{m}^2 \text{ K})$ (Figs. 1–4 and Table 1). This diffusivity is very close to the Knudsen diffusivity in a straight cylindrical pore of radius $r_p = 7.5 \text{ nm}$ [4] at $T = 90^\circ \text{C} = 363 \text{ K}$: $D_{kn} = 9700r_p \sqrt{T/M} = 3.3 \times 10^{-6} \text{ m}^2/\text{s}$. The diffusivity found in this work is approximately 10 times higher than that measured by a differential step method under isothermal conditions ($T = 35\text{--}70^\circ \text{C}$) for loose grains of SWS-1L $D_e = (0.24 \pm 0.12) \times 10^{-6} \text{ m}^2/\text{s}$ [13]. The efficient coefficient of heat transfer α_p obtained in this work is also higher than the one theoretically estimated. This estimation is based on the assumption that the main mechanism of heat transfer from the plate to the grain (or vice versa) is the heat conductance through the layer of a stagnant vapor,

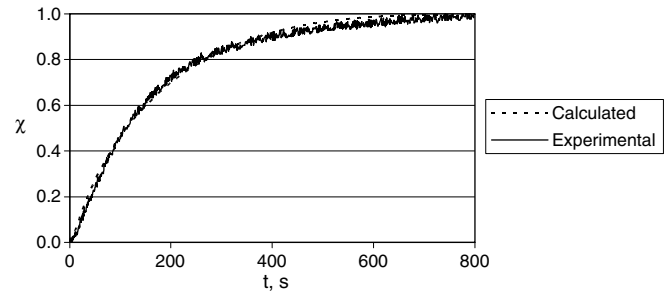


Fig. 1. Experimental (taken from [1], run 1) and calculated dimensionless uptake curves χ for water desorption from single grains of SWS-1L (1.4–1.6 mm size). Temperature jump $60^\circ \text{C} \Rightarrow 90^\circ \text{C}$, $P = 56.5 \text{ mbar}$, $D_e = 3 \times 10^{-6} \text{ m}^2/\text{s}$, $\alpha_p = 60 \text{ W}/(\text{m}^2 \text{ K})$.

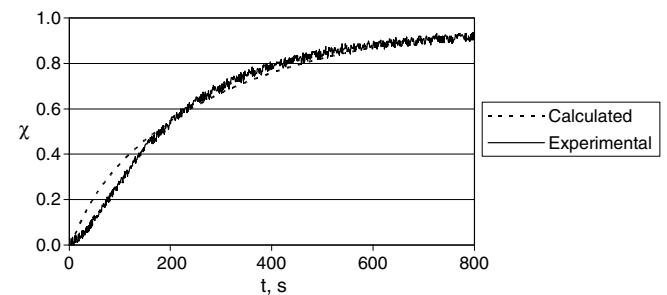


Fig. 2. Experimental (taken from [1], run 2) and calculated dimensionless uptake curves χ for water adsorption on single grains of SWS-1L (1.4–1.6 mm size). Temperature jump $90^\circ \text{C} \Rightarrow 60^\circ \text{C}$, $P = 56.5 \text{ mbar}$, $D_e = 3.0 \times 10^{-6} \text{ m}^2/\text{s}$, $\alpha_p = 60 \text{ W}/(\text{m}^2 \text{ K})$.

$\alpha_p = \lambda/R_p = 30\text{--}35 \text{ W}/(\text{m}^2 \text{ K})$, where $\lambda = 0.021 \text{ W}/(\text{m K})$ is the heat conductivity of water vapor at $T = 70^\circ \text{C}$ [14]. These differences in D_e and α_p indicate that under non-isothermal conditions the transfer of both heat and vapor can be more efficient than under quasi-equilibrium conditions. Possible reason of it could be an additional channel of the transfer due to a non-uniform temperature distribution that causes convective vapor flux towards colder sites in the system (a so called “heat pipe” or “recondensation” effect [15]), which enhances both heat and mass transfer.

The data for various runs shown in Table 1 demonstrate that the experimental and calculated characteristic times τ_c are in close agreement. It proves that the model accounts for major features of the experiments reported in [1]. In particular, the model confirms (a) the quasi-exponential shape of the uptake curves, (b) the finding that the adsorption process is always slower than the desorption one at the same temperature jump (Table 1 and Fig. 3). In [1] it was assumed, that this can be attributed to higher average grain temperature during desorption runs, due to the experimental fact that the average temperature of the metal plate reaches the temperature of the heat carrier (i.e., 90°C during desorption run 1 and 60°C during desorption run 2) within 1–2 min, yet the temperature of the isolated SWS grains was not measured during those experiments. To check this, we calculated the temporal evolution of the average grain temperature T_{av} for desorption and adsorp-

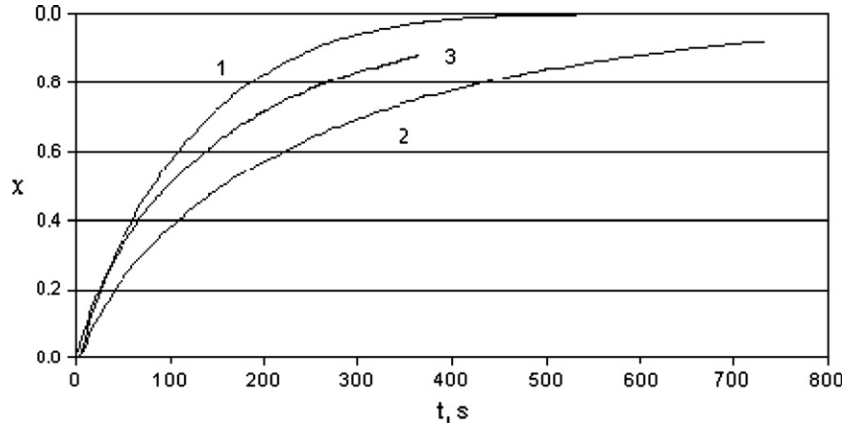


Fig. 3. Calculated dimensionless uptake curves χ for water desorption (curve 1) and adsorption (curve 2) which correspond to runs 5 and 6 [1]. Temperature jump $90\text{ }^{\circ}\text{C} \rightleftharpoons 80\text{ }^{\circ}\text{C}$, $P = 56.5\text{ mbar}$, $D_c = 3.0 \times 10^{-6}\text{ m}^2/\text{s}$, $\alpha_p = 60\text{ W}/(\text{m}^2\text{ K})$. Curve 3 corresponds to adsorption and desorption runs calculated for an artificial linear isobar of water sorption (see text).

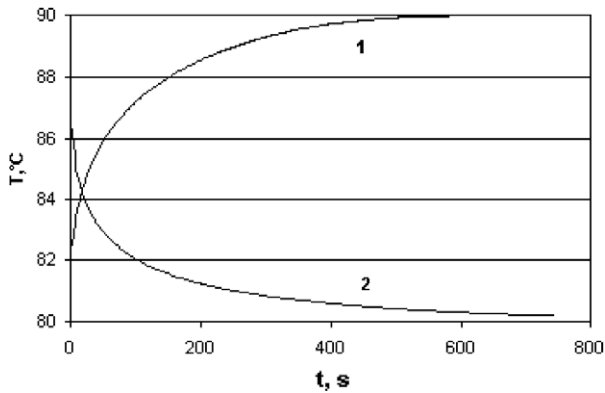


Fig. 4. Calculated dependence of the average grain temperature on time during desorption (1) and adsorption (2) for conditions corresponding to runs 5 and 6 in [1]. Temperature jump $90\text{ }^{\circ}\text{C} \rightleftharpoons 80\text{ }^{\circ}\text{C}$, $P = 56.5\text{ mbar}$, $D_c = 3.0 \times 10^{-6}\text{ m}^2/\text{s}$, $\alpha_p = 60\text{ W}/(\text{m}^2\text{ K})$.

Table 1
Experimental and calculated characteristic times τ_c and rate constants k of water sorption on the single grains of composite sorbent SWS-1L subjected to the temperature jump ΔT for several experimental runs [1]

Temperature jump ΔT , $^{\circ}\text{C}$ (run N)	Experiment		Model	
	τ_c (s)	k (s^{-1})	τ_c (s)	k (s^{-1})
<i>Adsorption</i>				
90–60 (run 2)	262	0.00382	266	0.00376
90–80 (6)	248	0.00403	247	0.00405
80–70 (7)	263	0.00380	251	0.00398
70–60 (8)	263	0.00380	244	0.00410
<i>Desorption</i>				
60–90 (1)	161	0.006211	166	0.00602
60–70 (3)	201	0.004975	225	0.00444
70–80 (4)	158	0.006329	233	0.00429
80–90 (5)	191	0.005236	134	0.00746

tion runs 5 and 6 (Fig. 4). These calculations showed faster initial change of T_{av} for adsorption run 5 than for desorption run 6 ($3.7\text{ }^{\circ}\text{C}$ instead of $2.5\text{ }^{\circ}\text{C}$ within the first 4 s).

Then, the rate of temperature change became slower during the adsorption run (Fig. 4). As a result, for desorption the grain temperature did reach the plate temperature in 6–7 min instead of 12–14 min for adsorption. Thus, during both the adsorption and desorption processes the grain temperature is essentially non-steady state that indicates the importance of the heat transfer from the plate to the grain at all times. The isothermal estimations of the adsorption/desorption rate done in [1] neglected this process and considered only the mass transport.

2.2. Dynamic behaviour and equilibrium sorption properties of the adsorbent

The interdependence between the heat and mass transfer can be more clearly seen if present the evolution of the grain state as “the average grain temperature T ” vs. “the average pressure inside the grain P_w ” (Fig. 5). For the jump $90\text{ }^{\circ}\text{C} \rightleftharpoons 80\text{ }^{\circ}\text{C}$ at $t = 0$ (point A) the driving force for heat transfer is maximum while the driving force for mass transfer equals 0. This initiates the fast cooling of the grain mentioned above (Fig. 4) that reduces the driving force for the heat transfer. Dropping the grain temperature stimulates the adsorption of water molecules first from the gas phase inside the pores. As the adsorption is fast, at short times the diffusional flux of vapor into the grain is not sufficient to compensate the pressure decrease. The pressure difference $P - P_w$ generates the driving force for mass transport which is increasing till point B (Fig. 5). The adsorption of water proceeds that results in the release of the adsorption heat inside the grain which slows down the temperature decrease and so on. Thus, the mass and heat transfer processes are inevitably coupled and strongly influence each other. At longer times, P_w is increasing due to the vapor flux from the outside into the grain, until the system reaches the equilibrium at point D at which the driving forces for both the heat and mass transfer become zero. During the reverse jump $80\text{ }^{\circ}\text{C} \rightleftharpoons 90\text{ }^{\circ}\text{C}$ the initial rise of the grain temperature initiates fast water desorption to

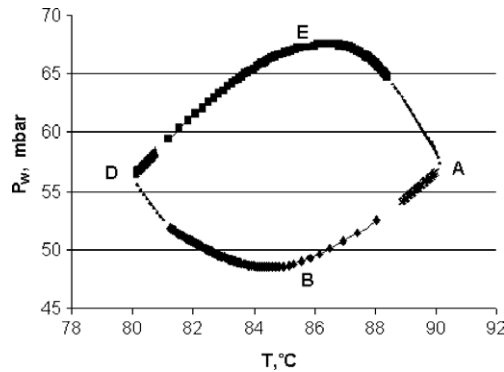


Fig. 5. Evolution of the average grain temperature T and the average pressure inside the grain P_w for the temperature jump between $90\text{ }^{\circ}\text{C}$ and $80\text{ }^{\circ}\text{C}$ and back (runs 6 and 5 [1]). A corresponds to the state of the system before the jump $90\text{ }^{\circ}\text{C} \Rightarrow 80\text{ }^{\circ}\text{C}$. Line ABD represents the process of the grain cooling which initiates the adsorption of vapor. D corresponds to the state of the system before the jump $80\text{ }^{\circ}\text{C} \Rightarrow 90\text{ }^{\circ}\text{C}$. Line DEA represents the process of the grain heating which initiates the desorption of vapor.

the pore space. This increases the heat consumption for the desorption process and make the grain heating much slower (Fig. 4). On the other hand, the desorption leads to the rise of P_w that causes the water flux from the grain.

The calculated values of the efficient specific heat $C = dQ/dT/M$ of the grain as a function of the average grain temperature are presented in Fig. 6. This value is the heat necessary for heating (cooling) the single grain of SWS-1L by $1\text{ }^{\circ}\text{C}$ related to its mass. It is much larger that the specific heat of silica ($0.73\text{ J}/(\text{g K})$), calcium chloride ($0.70\text{ J}/(\text{g K})$) and liquid water ($4.2\text{ J}/(\text{g K})$), because the heat is consumed mostly for desorption (adsorption) of water rather than for heating (cooling) the grain. The function $C(T)$ has a break at $T \approx 85.5\text{ }^{\circ}\text{C}$ (see the fragment on Fig. 6) for both the adsorption and desorption runs 5

and 6. It is interesting that at the same temperature there is a break on the isobar $N(T)$ of water sorption on SWS-1L (Fig. 7) at the average pressure during discussed experiments ($P = 56.5\text{ mbar}$). The plateau at $T > 85.5\text{ }^{\circ}\text{C}$ corresponds to the formation of $\text{CaCl}_2 \cdot 2\text{H}_2\text{O}$ with the almost constant water uptake $N \approx 2$. One can assume that the break of the function $C(T)$ is caused by the non-linear shape of the equilibrium isobar.

Indeed, during run 5 the majority of water is desorbed within the temperature range from 80.0 to $85.5\text{ }^{\circ}\text{C}$. At $T > 85.5\text{ }^{\circ}\text{C}$ the contribution of water desorption becomes much smaller; the $C(T)$ has the break and is slowly approaching the specific heat of the system ($\text{SiO}_2 + \text{CaCl}_2 \cdot 2\text{H}_2\text{O}$) $C = 1.2\text{ J}/(\text{g K})$. During the adsorption run 6 within the temperature range from 90.0 to $85.5\text{ }^{\circ}\text{C}$ there is almost no adsorption, see Fig. 7a, dN/dT is very small, $C(T)$ is smaller than $C(T)$ for desorption from 80.0 to $85.5\text{ }^{\circ}\text{C}$. And the average grain temperature changes faster than that during run 5. Fig. 5 does show that the grain reaches $T^{\text{av}} = 85.5\text{ }^{\circ}\text{C}$ much faster during the adsorption run. At $T^{\text{av}} < 85.5\text{ }^{\circ}\text{C}$ the adsorption starts, see Fig. 7a, the absolute value of the derivative dN/dT increases. When T^{av} is approaching $90\text{ }^{\circ}\text{C}$ the driving force for the heat transfer ($\Delta T = 90\text{ }^{\circ}\text{C} - T^{\text{av}}$) is getting smaller, while $[dN/dT]$ is continuously rising. This is probably the main reason why the adsorption has longer tail that the desorption, which results in larger characteristic times for adsorption runs.

In general, this should be true for any adsorbents with a concave shape of water sorption isobar. A linear sorption isobar should lead to equal kinetics of adsorption and desorption (Fig. 3, curve 3), while a convex shape like it is a case for SWS-1L at $P = 56.5\text{ mbar}$ at $T = 105\text{--}113\text{ }^{\circ}\text{C}$ (Fig. 7b) results in faster adsorption runs (Fig. 8). Thus, the dynamics of water adsorption on a single adsorbent

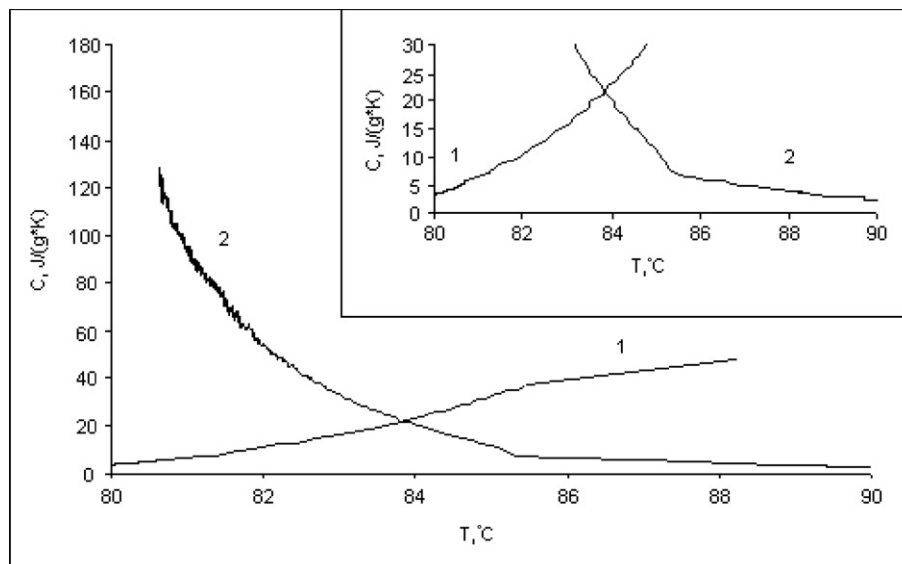


Fig. 6. Efficient specific heat of a single grain of SWS-1L as a function of the average grain temperature (1 – desorption run 5, 2 – adsorption run 6).

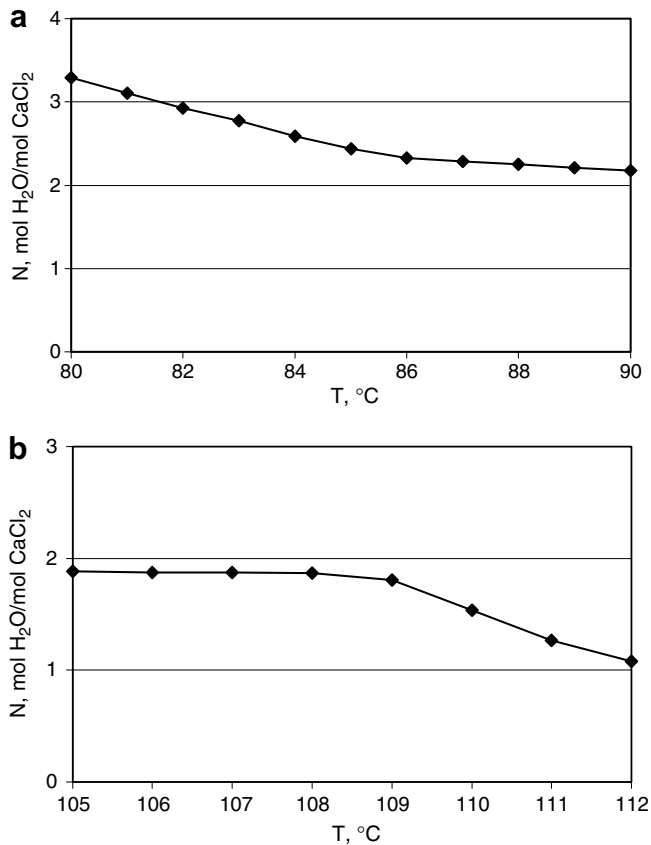


Fig. 7. Isobar of water sorption on SWS-1L at $P = 56.5$ mbar calculated according to the equilibrium equations reported in [11] in the temperature range 80–90 °C (a) and 105–113 °C (b).

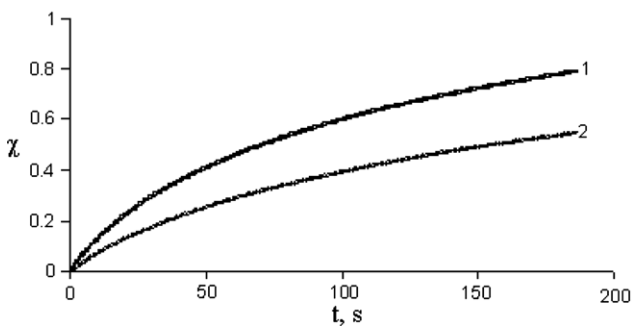


Fig. 8. Calculated dimensionless uptake curves for water adsorption (curve 1) and desorption (curve 2) which correspond to temperature jumps 105 °C \Leftrightarrow 113 °C. $P = 56.5$ mbar, $D_e = 3.0 \times 10^{-6}$ m²/s, $\alpha_p = 60$ W/(m² K).

grain is closely linked with equilibrium properties of the adsorbent, in particular, with the shape (convex, concave or linear) of the segment of water sorption isobar between the initial and final temperatures.

3. Conclusions

A new methodology of studying the kinetics of water vapour sorption/desorption under operating conditions

typical for isobaric stages of sorption heat pumps has been proposed and tested experimentally in [1]. Here, we analysed the results obtained by a mathematical modelling of the coupled heat and mass transfer in a single adsorbent grain which is in thermal contact with a metal plate subjected to a fast temperature jump/drop (at almost constant vapour pressure). Temporal evolution of the average pressure P_{av} inside the grain, its average temperature T_{av} and uptake χ were calculated. Despite of complex behaviour of $P_{av}(t)$ and $T_{av}(t)$, the uptake is found to be a quasi-exponential function of time. Characteristic times τ of isobaric adsorption/desorption calculated for single grain of composite sorbent SWS-1L (CaCl₂ in silica KSK) are in good agreement with those measured experimentally. The best fit corresponds to the water diffusivity $D_e = 3.0 \times 10^{-6}$ m²/s and the coefficient of the heat transfer between the plate and the grain $\alpha_p = 60$ W/(m² K). Dynamic behaviour is found to be closely linked with equilibrium properties of the adsorbent, in particular, with the shape of the segment of water sorption isobar between the initial and final temperatures.

Acknowledgements

This work was partially supported by INTAS (Grant 1 03-51-6260) and RFBR (Grant N 05-02-16953 and 05-03-34762).

References

- [1] Yu.I. Aristov, B. Dawoud, I.S. Glaznev, A. Elyas, A new methodology to study the kinetics of water vapour sorption/desorption under real operating conditions of adsorption heat pumps: 1. Experiment, Int. J. Heat Mass Transfer, submitted for publication.
- [2] R. Lang, M. Roth, M. Stricker, Development of a modular zeolite-water heat pump, in: Proceedings of International Sorption Heat Pump Conference ISHPC 99, Munich, Germany, March 24–26, 1999, 611–618.
- [3] B. Saha et al., Computer simulation of a silica gel-water adsorption refrigeration cycle – the influence of operating conditions on cooling output and COP, ASHRAE Trans.: Res. 101 (1995) 348.
- [4] D.M. Ruthven, Principles of Adsorption and Adsorption Processes, John Wiley and sons, New York, 1984.
- [5] A. Brunovska, V. Hlavacek, J. Ilavsky, J. Valtyni, An analysis of nonisothermal one-component sorption in a single adsorbent particle, Chem. Eng. Sci. 33 (1978) 1385.
- [6] A. Brunovska, V. Hlavacek, J. Ilavsky, J. Valtyni, Non isothermal one component sorption in a single adsorbent particle effect of external heat transfer, Chem. Eng. Sci. 35 (1980) 757.
- [7] R. Haul, H. Stremming, Nonisothermal sorption kinetics in porous adsorbents, J. Colloid Interface Sci. 97 (1984) 348.
- [8] L.M. Sun, F. Meunier, A detailed model for non-isothermal sorption in porous adsorbents, Chem. Eng. Sci. 42 (1987) 1585.
- [9] E. Yamamoto, F. Watanabe, N. Kobayashi, M. Hasatani, Intraparticle heat and mass transfer characteristics of water vapor adsorption, J. Chem. Eng. Jpn. 35 (1) (2002) 1–8.
- [10] Yu.I. Aristov, M.M. Tokarev, G. Cacciola, G. Restuccia, Specific heat and thermal conductivity of aqueous solutions of calcium chloride in silica pores, Rus. J. Phys. Chem. 71 (3) (1997) 391–394.
- [11] M.M. Tokarev, B.N. Okunev, M.S. Safonov, L.I. Heifets, Yu.I. Aristov, Approximation Equations for Describing the Sorption

- Equilibrium between Water Vapor and a CaCl_2 -in-Silica Gel Composite Sorbent, *Rus. J. Phys. Chem.* 79 (9) (2005) 1490–1494.
- [12] L.M. Sun, Y. Feng, M. Pons, Numerical investigation of adsorptive heat pump systems with thermal wave heat regeneration under uniform-pressure conditions, *Int. J. Heat Mass Transfer* 40 (2) (1997) 281–293.
- [13] Yu.I. Aristov, I.S. Glaznev, A. Freni, G. Restuccia, Kinetics of water sorption on SWS-1L (calcium chloride confined to mesoporous silica gel): Influence of grain size and temperature, *Chem. Eng. Sci.* 61 (5) (2006) 1453–1458.
- [14] J.Y. Andersson, H. Bjurstroem, M. Azoulay, B. Carlsson, Experimental and theoretical investigation of the kinetics of the sorption of water vapor by silica gel, *J. Chem.Soc., Faraday Trans.* 181 (1985) 2681–2692.
- [15] L.I. Heifets, D.M. Predtechenskaya, Yu.V. Pavlov, B.N. Okunev, Modeling of dynamic effects in the adsorbent beds. 1. Simple method to estimate thermal conductivity of the composite adsorbent bed (CaCl_2 , impregnated into pores of silica gel lattice), *Moscow Univ. Chem. Bull.* 61 (2006) 274–276.